A R C H I V E S O F M E T A L L U R G Y A N D M A T E R I A L S
Volume 50 2005 Issue 1

E.F. RAUCH*, L. DUPUY**

RAPID SPOT DIFFRACTION PATTERNS IDENTIFICATION THROUGH TEMPLATE MATCHING[1)]

SZYBKA IDENTYFIKACJA DYFRAKCYJNYCH OBRAZÓW PUNKTOWYCH ZA POMOCĄ DOBIERANEGO SZBLONU

The paper proposes a rapid method for diffraction patterns identification. It consists in comparing the acquired digital image of the spot pattern to a set of previously calculated templates. Image matching techniques are used to select the template with the highest correlation index. The procedure is used to measure automatically the microtexture of crystalline metallic materials.

W pracy przestawiono szybką metodę identyfikacji obrazu dyfrakcyjnego. Polega ona na porównywaniu uzyskanego obrazui cyfrowego dyfrakcji ze zbiorem wcześniej obliczonych obrazów dyfrakcyjnych. Jako metodę wyboru zastosowano technikę kojarzenia obrazów o największym współczynniku korelacji. Zaproponowaną procedurę użyto do automatycznego pomiaru mikrotekstury metalicznych materiałów krystalicznych.

1. Introduction

Diffraction patterns contain information on both crystallographic structure and orientation. It is therefore possible to map the material substructure by indexing point by point an extended area of the multi-crystalline sample. So called orientation maps can be constructed by scanning the area of interest, recording the diffraction patterns and identifying all the corresponding orientations. This enables features that are of prime importance for the mechanical properties of the material to be extracted such as grain size, local texture, twin boundaries or constitutive elements. The ease at which

* GENIE PHYSIQUE ET MECANIQUE DES MATERIAUX (CNRS-UMR5010) — INPG, B.P. 46, 38402 SAINT MARTIN D'HERES CEDEX FRANCE
** LAWRANCE LIVERMORE NATIONAL LABORATORY, L-415, LIVERMORE, CA 94550, USA
1) invited lecture

the orientations are identified is itself known to be correlated to the local state of the matter. Thus, grain boundaries, precipitates, recrystallized nuclei or even dislocation substructures may be indirectly detected with image quality indexes or similar parameters.

Among all the available techniques, Electron Backscatter Diffraction (EBSD) obtained with a scanning electron microscope (SEM) is undoubtedly the most widely used. Several commercial hardware and software systems are currently in operation and continuously improved. The Kikuchi patterns that are collected by the attached camera have a very good theoretical angular resolution, although the effective one is limited by the signal noise and is of the order of 0.5°. The spatial resolution has impressively decreased since first attempts from around 1μm down to less than 10 nm (1). This was of course made possible thanks to the implementation of field emission SEM.

Comparable procedures are less widespread on transmission electron microscopes (TEM). Both Kikuchi lines and spot patterns may be used to extract the crystallographic orientations (2-7). The fact that SEM tools are more advanced may be explained by the relative simplicity of SEM procedures. However, it should be mention that the increasing interest for nanomaterials constitute a strong driving force for the development of more accurate automates. TEMs have intrinsically the required spatial resolution and therefore intensive developments are expected in a near future to promote or improve fast and robust tools for automatic microtexture determination adapted to transmission electron microscopes.

It is the purpose of this paper to describe some simple solutions that can be used to develop such tools on existing TEMs. As mention above both Kikuchi or spot patterns may be consider to determine the crystal orientation and/or structure. Kikuchi lines are usually preferred presumably because they are known to lead to a more precise orientation measurement (6). The present project was initially concerned with severely deformed materials (8) that exhibit large internal stresses and high dislocation densities. Because in such cases the Kikuchi patterns are either weak or inexistent, the present computer indexing routines will only be concerned with the spot patterns. It will be stressed that the crystallographic orientation may be correctly identify even if the corresponding theoretical diffraction pattern is not perfectly recorded. Technical information and the indexing algorithm will be considered in turn in the following sections.

2. Hardware settings

A JEOL 3010 transmission electron microscope operating at 300 kV was fully equipped for the present purpose. The beam displacement is monitored by an external source via adequate connections on the deflector coils control boards. The remote computer contains a standard 12 bit D/A board delivering up to 10 volts on four filtered channels. The connection is performed after the beam tilt compensating stage

that is, for that reason, inactive. Consequently, while two channels control directly the beam x and y deflections, the two other may correct, if necessary, the beam tilt. Alternatively, the beam displacement may be controlled through the serial port of the inboard computer. However, the baud rate of such communication channels are too slow to enable the large number of data required for area scans to be collected. This latter procedure was also used, but only for line scans.

Digital pictures of the diffraction patterns are needed. Most of the recent TEMs are equipped with on-line digital cameras. Not all cameras allow long exposures in diffraction mode: the high intensity of the transmitted beam may easily damage permanently the sensor or merely lead to detrimental blooming. Moreover, the trend is to replace the traditional films by improving both the sensitivity and the resolution of CCD cameras. This means several million pixels and a dynamic range up to 16 bit. Consequently the exposure times are rather long, while high acquisition rates are required for the present purpose. By contrast, a spot pattern is reasonably rendered with a picture size as low as 128×128 pixels. A deep dynamic range would be beneficial because it facilitates indexing. Indeed, recognizing the faint diffracted beams related to larger Bragg angles improve significantly the angular resolution. However, to speed up the acquisition step, an 8 bit readout is preferred and appears quite sufficient.

The electron microscope is equipped with a GATAN Dualview 780 camera. Binning of 4 or 8 is used to reduced the 1300×1030 pixels down to the adequate resolution and the frame grabber is connected to the CCD controller 8 bit video output. The acquisition rate is typically 10 frames per second. The use of an external camera was tested as well and appeared to give appreciable results. This particular setting and the corresponding results will be described in a separate paper.

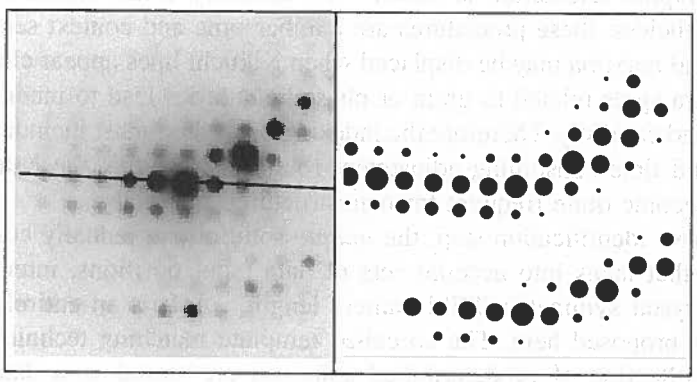

(a) (b)

Fig. 1. (a) Diffraction patterns acquired with the on-line digital camera and (b) the corresponding template (see section 3 for details). The material has a f.c.c. crystallographic structure. The beam direction is at 6° from [100] axis. The pixel intensities are inverted to enhance the apparent contrast of the weaker spots

Thousands of pictures are recorded for each orientation map. While the image processing and identification times would enable on-line calculations of the relevant parameters, it is preferred to store the data and process them afterwards. At the current step of the tool development, this permits the procedure to be optimized off-line by testing different identification algorithms. To scan an area of 100×100 pixels, it takes typically less than half an hour and the data will represent around two hundred megabytes.

As may be seen in Fig. 1.a, several spots appear more or less clearly on the picture. They are all characterized by their relative positions but also by their intensities. For a specified material and for known observation conditions there is only one orientation that corresponds to a given pattern. This simple fact is exploited in the identification process described below.

3. Indexing spot diffraction patterns

The usual scheme for indexing spot patterns with an automate reproduces the manual method. This means locating the intense spots (by digital image processing), computing the length and angles of the diffraction vectors to determine their families and, finally, identifying and reconstructing the crystal orientation by solving compatibility equations that stand for some geometrical rules between the indexed spots. The superiority of numerical approaches are the identification speed, of course, but also the possibility to increase the angular resolution by taking into account the spot intensities. This is illustrated in figure 1 where, thanks to the points that are far from the centre, the crystallographic orientation is known with accuracy better than a fraction of one degree. Nevertheless, these procedures are cumbersome and context sensitive. For instance, the local maxima may be displaced when Kikuchi lines appear close to the spot. Moreover, extra spots related to grain or phase boundaries lead to inconsistencies that must be handled carefully. Therefore the indexing procedure must include some degrees of freedom and time-consuming adjustment routines. Note that the latter difficulty is expected to become quite frequent for nanostructured materials.

In the above identification step, the *unique* solution is gradually constructed with an algorithm that takes into account sets of data (spot positions, intensities, ...) and constraints (crystal symmetry, TEM camera length, ...). It is an entirely different approach that is proposed here. The so called template matching technique (9-10) will be used. A collection of predetermined solutions are stored in a database and the best one is extracted through image correlations. The efficiency of the method is due to the fact that not more than two thousand templates are sufficient for an angular resolution better than 1°. Moreover, a template contains a limited number of points, each being characterized by three information: x and y coordinates as well as the intensity. Therefore, the image matching calculation is quite fast. Templates generation and the identification procedure will be described in the following.

3.1. Templates generation

It should first be mentioned that the theoretical diffraction patterns (the templates) can be generated in different ways without affecting the subsequent identification routine. Complete dynamical or kinematical calculations may be considered. It was preferred to keep the approach as simple as possible. Therefore, the classical geometric construction based on the Ewald sphere is applied. The procedure is quite similar to the pattern generation used by Zaefferer (6) to display, after indexing, the result for comparison purposes with the experimental picture. Each diffraction pattern is merely considered as the intersection of the reciprocal lattice with a sphere whose diameter is the inverse of the electron wavelength. Each dot in the reciprocal lattice is replaced by a rod whose length is such that the diffracting beam is seen (the sphere intersected) while the orientation or the associated lattice plane is slightly away from the Bragg angle. This permits the position of the diffracting beam to be calculated easily and quite accurately (Fig. 2).

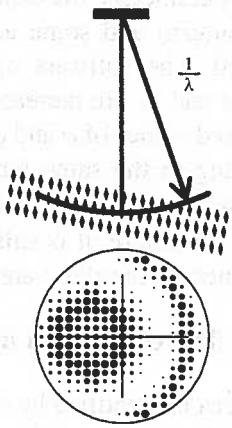

Fig. 2. Schematic view of the template construction. The shape of the nodes in the reciprocal lattice (upper part) is elongated along the beam axis in order to take into account the decrease of the spot intensity with increasing deviation from the Bragg condition (linear in this case). For display purpose, the disk diameter in the diffraction pattern is set proportional to the corresponding intensity (lower part). The overall size of the diffraction pattern is limited by the circle whose radius is determined empirically

The spot intensity depends on the distance between the diffracting beam and the transmitted beam (through the atomic scattering factor), the deviation from the Bragg angle, but also on observation conditions (two or multi- beams, foil thickness). Because the latter are not perfectly known especially for severely deformed materials, a precise calculation is hopeless. However, an exact value of the spot intensity is not necessary for orientation identification. An estimate is sufficient. This estimate is obtained by reducing the intensity linearly with the excitation error s (i.e., the deviation from the Bragg angle). Note that a more complex relationship (inverse, square root, exponen-

tial, ...) may be used as well without modification of the subsequent steps of the procedure. The result is illustrated in Fig. 2 where the disk diameters stand for the beam intensities. It is worth recalling that in the database, there are no disks, only triplets containing the coordinates and the intensity values. The excitation error used to reproduce reasonably the patterns is usually quite high: typically between 0.05 and 0.1Å^{-1}.

When the resulting template is compared to the experimental data (e.g. Fig. 1) clear discrepancies appear at the outer ring. The calculated intensities are higher than the real ones. This is because the progressive decrease of the atomic scattering factor with increasing Bragg angle is not considered here. An adjustment could be performed but, as will be stressed in the following section, this correction should *not* be introduced for the present purpose. In place, the radius or the template is bounded, i.e. only the diffracting beams having Bragg angles lower than a threshold value are considered. This radius is fitted to the acquire picture size.

The database is produced off-line by deduced software. The material characteristics (crystallographic structure, lattice parameter), the experimental conditions (accelerating voltage, size of the diffraction pattern) and some adjusted features (excitation error, angular resolution) are introduced. The software calculates the templates for every orientation, i.e., the Euler angles ϕ and ϕ_2 are increased step by step in ranges bounded by the symmetry of the crystal. Fixed values of ϕ and ϕ_2 give rise to a family of patterns. Two individual templates belonging to the same family and which are characterized by the angles ϕ_1 and ϕ_1' respectively may be deduced from each other by the rotation $(\phi_1' - \phi_1)$ around the normal axis. Therefore, it is sufficient to store one set of data per family. Typically around 1400 patterns (families) are generated for cubic materials.

3.2. The correlation index

Basically, the diffraction pattern is identified by calculating the degree of matching between the templates and the acquired data and by selecting the one with the highest index. The value of this index is the image correlation defined as follows: consider a pattern represented by the intensity function P(x,y) where x and y are bounded by the picture width and height respectively, for every individual template $T_i(x,y,\phi_1)$ corresponding to a rotation ϕ_1 of the template i taken among the N families stored in the database ($\phi_1 \in \{1°, 360°\}$, $i \in \{1, N\}$), the correlation index Q is:

$$Q(i,\phi_1) = \frac{\sum_{j=1}^{m} P(x_j,y_j)T_i(x_j,y_j,\phi_1)}{\sqrt{\sum_{j=1}^{m} P^2(x_j,y_j)}\sqrt{\sum_{j=1}^{m} T_i^2(x_j,y_j,\phi_1)}} \quad (1)$$

The summation should be performed for every pixel of the image ($m \approx 2.10^4$). But because the template is zero everywhere except for a very limited number of points, the calculation is drastically reduced: typically only 50 to 100 products are added. For each

template, the uppermost value among the ones corresponding to all the rotations ϕ_1 is stored in the family index $Q_m(i)$. Finally, the most probable orientation corresponds to the highest $Q_m(i)$.

The essence of the matching process is illustrated with a 1D example in figure 3: the intensity distribution is measured under the nearly horizontal line drawn in Fig. 1.a that passes exactly over intense and aligned spots. The discrete values are the corresponding estimates taken from the selected template (Fig. 1.b). The correlation between these two reduced sets of data is entirely characterized by summing nine products, i.e.: the discrete peak values times the corresponding measured intensities (the transmitted beam is omitted). It is worth noting that the correlation is high essentially because the intensity peaks are at the adequate positions. By contrast, the intensities are poorly rendered by the template, especially at large distance from the transmitted beam. As mentioned previously, this is mainly due to the absence of the atomic scattering correction. Introducing such an adjustment would lead to a better agreement. However, the contribution to the correlation index of the spots located at the outer ring of the diffraction patterns would decrease. It had appeared that this correction reduces both the quality of the identification and the angular resolution. It is therefore preferred to amplify the weight of the outer spots by merely omitting the atomic scattering factor. In fact, the reverse may be performed to improve indexing, i.e.: central spots may be artificially reduced. This increases the angular resolution but works only when the background noise is low (integrated pictures).

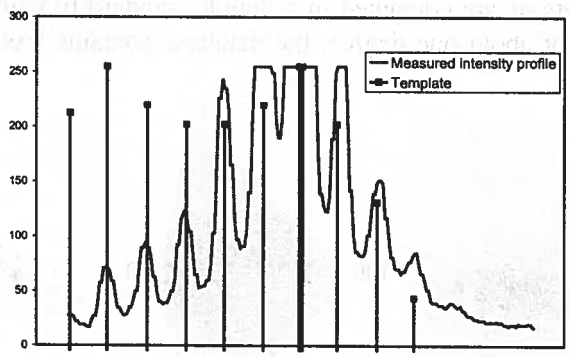

Fig. 3. One dimensional illustration of the matching process: the intensity profile (continuous curve) measured on the diffraction pattern is correlated to discrete points that belong to a template. The correlation index is the sum of the products related to the non zero values of this template

The main advantages of this strategy are listed below:

(i) there is no need to determine the positions or the intensities of the diffracting beams. This information will automatically be obtained by the matching process,

(ii) extra spots are excluded naturally from the calculation when the index of a template is estimated,

(iii) superimposed patterns (as at grain boundaries) are resolved because the predominant template will be selected (see section 4.1)

(iv) processing rate is fast

(iv) indexing time is identical for every orientation (every scanned point of the crystal)

(v) the identification algorithm does not depend on the crystallographic structure. Only the template generating software needs to be adapted.

(vi) for low symmetry materials, the processing time is only moderately increased (e.g., by a factor of two for h.c.p. materials).

3.3. The correlation indexes map

The orientation identification scheme is illustrated on Fig. 4 where a spot diffraction pattern related to a nanocrystalline copper thin foil is shown. Because for a small object the sample cannot be tilted without loosing the area of interest, the orientation of the crystal is most of the time out of well defined zone axes. The pattern is first numerically transformed. The objective of the image processing step is twofold: firstly it is essential to locate properly the transmitted beam and secondly the background intensity should be subtracted to enhance the spot contrast (compare Fig. 4.c to 4.a). Then, the correlation index is estimated for every pre-calculated template. These templates are dedicated to the specific observation conditions (electron wavelength, camera length, lattice parameter, crystallographic structure). For cubic materials all the possible and distinct orientations are contained in a double standard triangle (Fig. 4.b). For an angular resolution of about one degree, the database contains less than two thousand patterns.

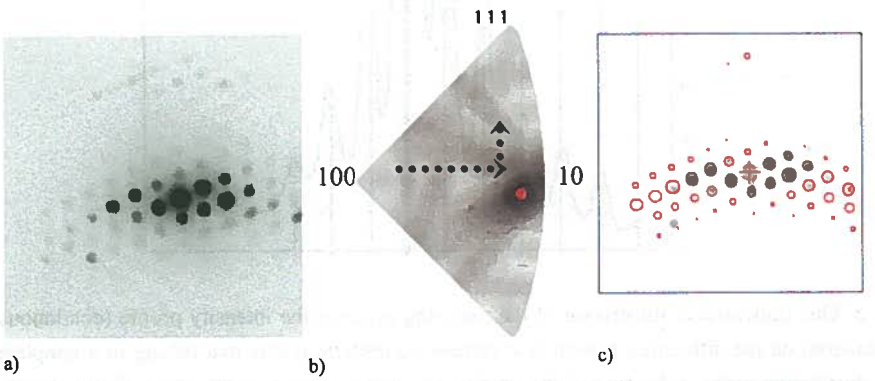

Fig. 4. The selected diffraction pattern (left) is compared to the templates that are calculated for every possible orientation. The highest correlation index, denoted by the grey level in the *correlation indexes map* (center), is selected and the associated template is shown superimposed on the pattern transformed by image processing (right). The pattern refers to a copper nanocrystalline thin foil

The correlation indexes being estimated for every single orientation, they may be compared by plotting their values in grey levels on the standard triangles. The resulting

correlation indexes map (Fig. 4.b) appears quite useful to locate visually the proposed orientation. In this map the indexes are normalized by the highest value (black). It is obvious that there is no other possible solution for the given pattern than the ones that are in the close vicinity of the selected one. The agreement may be inferred from Fig. 4.c where the proposed solution is superimposed on the pre-processed diffraction pattern.

3.4. The reliability index

The main drawback with template matching is that there is always a solution. Indeed, the selected template is the best one, but this does not mean that it is a good one. Fundamentally, the correlation index measures a quantitative agreement between the theoretical and the experimental images. It does not weight properly the quality of the identification. By construction, the index Q is lower than 1. If Q approach this upper limit (for nearly identical images) the quality of the matching may be characterized by the quantity Q. By contrast, the very limited number of dots in the present templates makes this value very low ($Q < 10^{-3}$) and more sensitive to the pattern contrast than to the identification quality. Similar correlation indexes may be obtained either when a well contrasted pattern is poorly recognized (e.g.: second phase particle) or when the matching is correct but the background noise is important (thick samples). Consequently, a quality index must be derived.

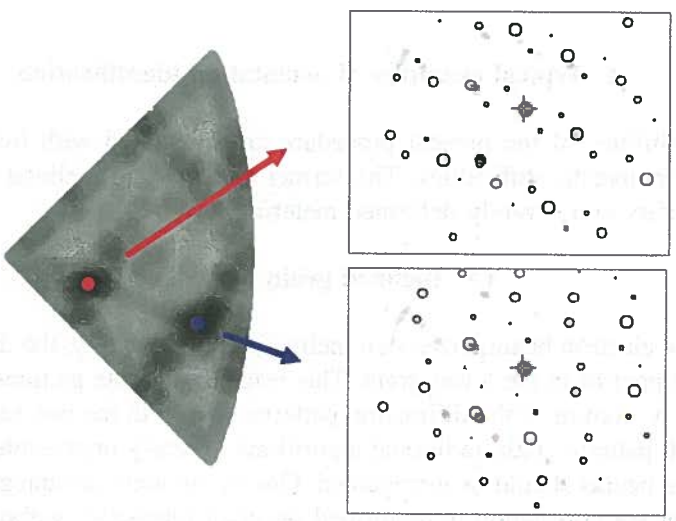

Fig. 5. The selected template is the upper right one. An ambiguity arises from the existence of another solution (lower right) with a similar correlation index (136 with respect to 140). The poor reliability of the indexing is evident on the correlation indexes map (left). The reliabiliy index is equal to 4

Figure 5 gives an example of an ambiguity that arises when the acquired diffraction pattern has a limited amount of information. Two solutions are proposed with nearly

equal correlation indexes and therefore the proposed orientation should be rejected. The poor quality of the indexing is apparent on the associated correlation indexes map. Indeed, several maxima are easily seen and each of them corresponds to a different solution. This indistinctness may be weighted by considering the ratio of the two highest maxima seen on that map. More precisely a reliability index is defined as follows:

$$R = 100\left(1 - \frac{Q_2}{Q_1}\right) \tag{2}$$

where Q_1 and Q_2 stand for the two highest values of the correlation indexes for distinct maxima. Basically the reliability is null if the two solutions are equivalent and R tends toward 100 when the second solution (Q_2) is relatively low compared to the first one (Q_1). From a practical point of view, the proposed orientation is safe if R is higher than 15, it is excellent for a reliability index higher than 40.

Values of R are frequently low. Up to 30% of the data have reliability indexes lower than 15. This is partly due to the fact that for the sake of rapidity, the acquisition time is reduced at the expense of the pattern quality. But mainly the Bragg angles captured by the spot patterns is limited and the quantity of information contained in the area of the diffraction pattern that is far from the transmitted beam is frequently quite poor. This leads to ambiguities that reduce the reliability index. This limitation is particularly important for spot patterns. Acquisition or indexing strategies that reduce or correct this drawback are currently under development.

4. Typical examples of orientation identification

The capabilities of the present procedure are illustrated with two cases that are known to have specific difficulties. The former concerns an inclined grain boundary, the second refers to a severely deformed material.

4.1. Inclined grain boundary

When the electron beam crosses an inclined grain boundary, the diffraction occurs either in the upper or in the lower grain. This leads to intricate pictures that are mainly composed of a mixture of the diffraction patterns related to the two separated crystals. Indexing such patterns with traditional algorithms is nearly impossible: around half of the diffracting beams should be disregarded. One of the main advantages of the present routine is that the correlation is performed on pixel intensities without any reference to the fact that these intensities are related to definite Bragg conditions. Therefore, the correspondence between the pattern and the template is estimated whatever the quality of the former. In particular, when two distinct diffraction patterns are mixed in a simple picture, *both* orientations are proposed as potential solutions. This specific behavior of the template matching technique is illustrated on figure 6 where and inclined grain boundary is considered. The diffraction patterns belonging to the two isolated grains

are shown on Fig. 4 (grain 1) and Fig. 6.c (grain 2) respectively. For intermediate positions (Fig. 6.a and b) and despite the complex aspect of the pattern, either the left grain (Fig. 6.a) or the right grain (Fig. 6.b) is selected. It should be noted that while the related correlation indexes maps exhibit the maximum at the adequate locations (near [110] and [211] respectively), information belonging to the other grain is also apparent on the maps (e.g.; dark area near [110] on Fig. 6.b and vice versa).

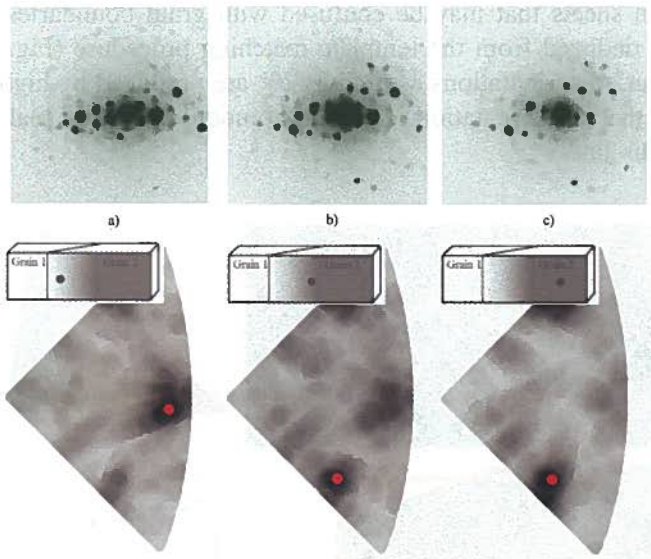

Fig. 6. Superimposed diffraction patterns (upper) and related *Correlation indexes maps* (lower). When an inclined grain boundary is crossed by the electron beam (a and b), diffraction spots related to grain 1 (figure 4) and grain 2 (Fig. 6.c) are mixed. In all cases, the process is able to resolve the problem by selecting the best solution (see text for details)

It is worth mentioning that for a given foil thickness, the probability to encounter mixed diffraction patterns is increasing with decreasing grain size. For nanoscaled materials this situation is expected to become of major concern if the crystallographic orientation is required.

4.2. Severely deformed low carbon steel

While EBSD tools are undoubtedly very efficient to derive orientation maps with impressive spatial resolution when they are coupled to a SEM-FEG, they still experience some difficulties when the level of strain is increase. This results from the poor quality of the Kikuchi patterns when the crystals contain a high density of defects. The same is observed for TEM Kikuchi patterns. Because the Kikuchi lines are very sensitive to the crystal orientation, they rapidly fade away if the diffracting volume suffers distorsions. By contrast, these distorsions will have a limited effect on the spot

patterns: indeed, small misorientations will affect the intensity and not the position of the diffracted beams. In other words, the related spots will appear on the diffraction pattern even if the beam has crossed a volume whose orientation is broadened. The aptitude of the spot patterns to measure the local orientation for a severely deformed material is shown on figure 7. A low carbon steel was subjected to cyclic planar simple shear test. Each complete cycle corresponds to a cumulated shear strain of 1.8 and the sample was cycled 10 times. The resulting substructure is composed of sharp dislocation sheets that may be confused with grain boundaries (Fig. 7.b). The orientation map deduced from the template matching procedure (Fig. 7.a) shows that along a 4 μm line, misorientations as high as 20° are produced by high levels of strain (Fig. 7.c). Note that the orientation is gradually modified and no real grain boundary appears along this line.

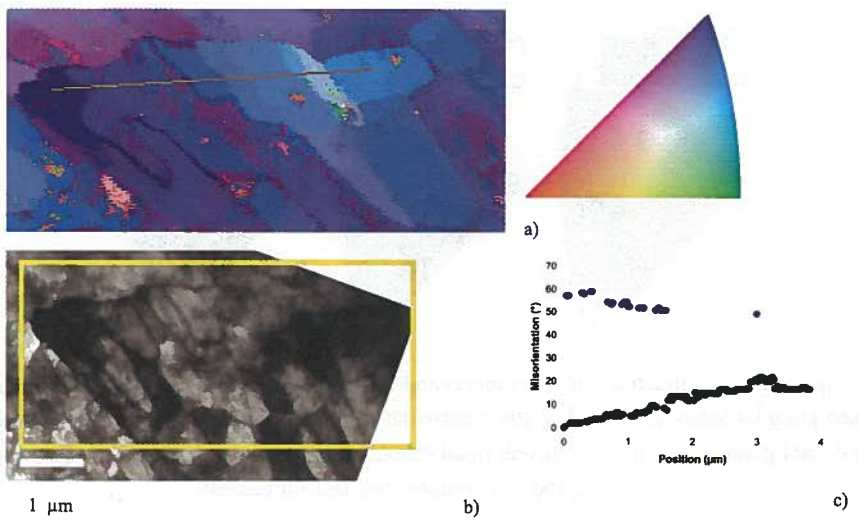

Fig. 7. Low carbon steel deformed in alternated shear to a total strain of γ = 18.3. The orientation map (a) demonstrated that despite an overall polycrystalline aspect of the area (b) the whole volume bears a unique global [111] orientation. By contrast, misorientations within the area (line denoted on (a)) are important and progressive. The map size is 6×2.6 μm and was scanned by individual steps of 20 nm

It appears from the misorientation plot (Fig. 7.c) that abnormal values are frequently obtained. This is partly due to the fact that the calculation is made for rough data (i.e.: the orientation map was not cleaned or eroded) but mainly local jumps of around 60o are related to orientation ambiguities. The latter are particularly observed in the vicinity of the high symmetry poles (e.g. the nearly perfect [111] orientation at the left part of the plot) and especially when the outer part of the diffraction pattern does not provide sufficient information. Despite this limitation, the orientation maps demonstrate the capability of the present tool to deal with highly strained samples.

5. Conclusions

A new tool that permits to determine automatically crystallographic orientations maps at a submicron scale is presented. The procedure takes advantage of the high spatial resolution of transmission electron microscopes. While the area of interest is scanned through an external control of the beam displacement, the diffraction patterns are collected with a digital camera and analysed with dedicated software. The numerical identification is performed thanks to a fast algorithm that consists in mapping the diffraction spots with pre-calculated patterns. Measurements of local misorientations or gradients of orientation are performed with a spatial resolution only limited by the beam size (<10nm).

REFERENCES

[1] D. Dingley, J. of Microscopy **213/3**, 214-224 (2004).
[2] R.A. Schwarzer, Textures and Microstructures **13**, 15-30 (1990).
[3] S. Zaefferer, R.A. Schwarzer, Z. Metallkunde **85**, 585-591 (1994).
[4] R.A. Schwarze, J. Sukkau, Mater. Sci. Forum **273-275**, 215-222 (1998).
[5] A. Morawiec, J. Appl. Cryst. **32**, 788-798 (1999).
[6] S. Zaefferer, J. Appl. Cryst. **33**, 10 (2000).
[7] J.-J. Fundenberger, A. Morawiec, E. Bouzy, J.S. Lecomte, Ultramicroscopy **96**, 127-137 (2003).
[8] L. Dupuy, E.F. Rauch, J.J. Blandin, 'Texture, Structural Evolution And Mechanical Properties In AA5083 Processed By Ecae', in *Investigations and Applications of Severe Plastic Deformation*, T. C. Lowe and R.Z. Valiev (eds), Kluwer Academic Publishers, 189-195 Netherlands, (2000).
[9] W.K. Pratt, Digital Image Processing, Wiley, New York, 1978.
[10] A. Rosenfeld, A.C. Kak, Digital Picture Processing, Computer Science and Applied Mathematics, Academic Press, New York, 1976.

Received: 24 January 2005.